Human Molecular Genetics, 2010, Vol. 19, No. 23 **4663–4676**
doi:10.1093/hmg/ddq397
Advance Access published on September 14, 2010

The planar cell polarity gene *Vangl2* is required for mammalian kidney-branching morphogenesis and glomerular maturation

Laura L. Yates[1,†], Jenny Papakrivopoulou[2,3,†], David A. Long[2], Paraskevi Goggolidou[1], John O. Connolly[3], Adrian S. Woolf[4] and Charlotte H. Dean[1,*]

[1]Mammalian Genetics Unit, Medical Research Council, Harwell, Oxfordshire OX11 0RD, UK, [2]Nephro-Urology Unit, UCL Institute of Child Health, London, UK, [3]UCL Centre for Nephrology, Royal Free and University College Medical School, London, UK and [4]University of Manchester and Royal Manchester Children's Hospital, Manchester, UK

Received July 28, 2010; Revised and Accepted September 8, 2010

The planar cell polarity (PCP) pathway, incorporating non-canonical Wnt signalling, controls embryonic convergent (CE) extension, polarized cell division and ciliary orientation. It also limits diameters of differentiating renal tubules, with mutation of certain components of the pathway causing cystic kidneys. Mutations in mouse *Vangl* genes encoding core PCP proteins cause neural tube defects (NTDs) and *Vangl2* mutations also impair branching of embryonic mouse lung airways. Embryonic metanephric kidneys also undergo branching morphogenesis and *Vangl2* is known to be expressed in ureteric bud/collecting duct and metanephric mesenchymal/nephron lineages. These observations led us to investigate metanephroi in *Vangl2* mutant mice, *Loop-tail* (*Lp*). Although ureteric bud formation is normal in *Vangl2*$^{Lp/Lp}$ embryos, subsequent *in vivo* and *in vitro* branching morphogenesis is impaired. Null mutant kidneys are short, consistent with a CE defect. Differentiating glomerular epithelia express several PCP genes (*Vangl1/2*, *Celsr1*, *Scrib, Mpk1/2* and *Fat4*) and glomeruli in *Vangl2*$^{Lp/Lp}$ fetuses are smaller and contain less prominent capillary loops than wild-type littermates. Furthermore, *Vangl2*$^{Lp/+}$ kidneys had modest reduction in glomerular numbers postnatally. *Vangl2*$^{Lp/Lp}$ metanephroi contained occasional dilated tubules but no overt cystic phenotype. These data show for the first time that a PCP gene is required for normal morphogenesis of both the ureteric bud and metanephric mesenchyme-derived structures. It has long been recognized that certain individuals with NTDs are born with malformed kidneys, and recent studies have discovered *VANGL* mutations in some NTD patients. On the basis of our mutant mouse study, we suggest that PCP pathway mutations should be sought when NTD and renal malformation co-exist.

INTRODUCTION

The planar cell polarity (PCP) pathway, incorporating non-canonical Wnt signalling (1,2), directs embryonic convergent (CE) extension, polarized cell division and cell differentiation and also orientates cilia (3–6). *Vangl* (*Van Gough/Strabismus*) genes code for core PCP proteins. The transmembrane protein Vangl2 is expressed in the embryonic neural tube (7) and the mouse *Loop-tail* (*Lp*) allele comprises a *Vangl2* mutation which encodes an unstable and mislocalized, and thus non-functional, protein product (8,9). The mutation is 'semi-dominant' with heterozygous mice being overtly healthy but characterized by their malformed tails; *Vangl2*$^{Lp/Lp}$, however, causes a severe neural tube defect (NTD) called craniorachischisis (10). In this context, the normal function of Vangl2 is to facilitate, via Rho kinase (ROCK) and cytoskeletal rearrangement, cell-autonomous CE in axial mesoderm and neuroepithelium before neurulation (11). *Vangl1*^{gt}/*Vangl2*^{Lp} compound heterozygous mice have severe NTDs (12) and subsets of individuals born with NTDs have been

*To whom correspondence should be addressed at: Tel: +44 1235841100; Fax: +44 1235841282; Email: c.dean@har.mrc.ac.uk
†The authors wish it to be known that, in their opinion, the first two authors should be regarded as joint First Authors.

reported to have either *VANGL1* or *VANGL2* variants (13–16) which may lead to dysfunctional gene products and thus contribute to the pathogenesis of neural defects (17). Genetic experiments in mice and zebrafish have shown that Vangl2 functions together with centrosomal/basal body-associated proteins, mutated in the Bardet–Beidl (18) and oral facial digital (19) syndromes, to drive embryonic CE. Furthermore, Vangl2 directs the orientation of primary cilia, thus allowing them to function optimally (5,6,20).

The embryonic precursor of the metanephros, which differentiates into the mature mammalian kidney, initiates around the fifth week of human gestation and embryonic day 11 (E11) in mice (21,22). The first phase of its morphogenesis is dominated by epithelial branching, starting with the outgrowth of the ureteric bud from the mesonephric duct, followed by arborization of the bud into the collecting ducts which drain forming urine into the renal pelvis from where it enters the ureter (21). Near the branching tips, metanephric mesenchyme converts into another epithelium, the nephron vesicle, which subsequently segments, elongates and differentiates into components including the glomerular podocytes, cells involved in ultrafiltration of blood in the first step of urine production (23,24), and the proximal tubules featuring actin-rich apical brush borders (25) which modify the ultrafiltrate by reabsorption of specific molecules.

The embryonic lung is another organ which forms by branching morphogenesis, and we recently reported that *Vangl2*$^{Lp/Lp}$ mice have defective embryonic lung airway branching (26). Lung branching was also perturbed in *Crash* mice which have mutation of *cadherin EGF LAG seven pass G-type receptor 1/Flamingo* (*Celsr1*), another gene encoding a PCP protein (26). Intriguingly, in murine developing kidneys, Vangl2 protein is known to be expressed in ureteric bud epithelia (7) and in fetal podocytes (27). Although the exact pattern of branching is different in kidneys and lungs, the above observations led us to hypothesize that Vangl2 may have roles in kidney-branching morphogenesis and perhaps glomerular maturation. On the basis of the results of our current *Vangl2* mutant mouse study, which indeed show that this PCP component is required for normal kidney morphogenesis, we suggest that *VANGL* mutations should especially be sought in humans who are found to have both an NTD and a malformed renal tract (28–30).

RESULTS

Branching morphogenesis is disrupted in *Vangl2*^{Lp} kidneys *in vivo* and *in vitro*

To determine whether kidney development was affected by *Vangl2* mutation, we first examined the anatomical initiation of the metanephros. In transverse sections of both wild-type and *Vangl2*$^{Lp/Lp}$ E11.5 embryos, we observed paired metanephric rudiments, each with a ureteric bud surrounded by mesenchymal cells (Fig. 1A and B). By E13.5, the normal ureteric bud has branched several times (21,22). Whole-mount immunostaining for cytokeratin was undertaken (Fig. 1C and D) to visualize both branching tips and collecting duct stalks (31). E13.5 wild-type organs contained significantly more ureteric bud branch tips than either heterozygous or homozygous *Vangl2 mutant* E13.5 metanephroi (Fig. 1E). None of the several tens of mutant embryos examined between E11 and late gestation had other ureteric defects such as duplication or dilatation (data not shown). We noted that both at E13.5 and in later gestation (E18.5) *Vangl2*$^{Lp/lp}$ kidneys appeared smaller compared with wild-type littermates, especially in their antero-posterior axis (Fig. 1C, D and F). In fact, homozygous mutant E18.5 kidneys had a significantly ($P < 0.01$) lower length/width ratio (mean $\pm$ SEM; 1.48 ± 0.02, $n = 3$) than wild-type organs (1.74 ± 0.02, $n = 3$). *Vangl2*$^{Lp/Lp}$ embryos are known to have a shortened rostrocaudal axis, and this has been attributed to a primary CE defect (11). Thus, a trivial explanation for the small mutant metanephroi would be that, *in vivo*, an abnormally shaped embryonic body might have physically constrained their morphogenesis. We therefore isolated late E11.5 metanephroi and followed their progress in serum-free organ culture (32). After 2 days, wild-type organs had undergone marked growth (Fig. 1G) whereas, in comparison, the progress of *Vangl2*$^{Lp/Lp}$ organs appeared retarded to variable degrees (Fig. 1H and I). At this stage, wild-types had significantly more ureteric bud branch tips versus *Vangl2*$^{Lp/Lp}$ organs (Fig. 1J). In other experiments, E12 organs, in which the bud had branched once, were cultured for 5 days and then co-immunostained for cytokeratin, to highlight the ureteric bud lineage, and Wilms tumour 1 (WT-1), to highlight glomerular podocytes (33) (Fig. 1K and L). At the end of the observation period, *Vangl2*$^{Lp/Lp}$ organs always appeared smaller than wild-type metanephroi (Fig. 1K and L). Mutant kidneys *in vitro* contained branch tips which frequently appeared distorted and wider than normal (compare Fig. 1 inserts in C and D and also frames K and L); we have previously noted a similar phenotype in the lungs of *Vangl2*$^{Lp/Lp}$ mice (26). Cultured organs from both genotypes contained clusters of WT-1-expressing cells, indicating that lack of Vangl2 function did not block formation of glomeruli *in vitro* (Fig. 1K and L). The detailed effects of *Vangl2* mutation on glomerular maturation *in vivo* are explored below.

The late-gestation *Vangl2*$^{Lp/Lp}$ kidney has poor cortico-medullary definition, a hypoplastic medulla and mildly dysmorphic tubules

At E14.5, homozygous mutant metanephroi appeared smaller than those of wild-types (Fig. 2A–C). Inside E14.5 *Vangl2*$^{Lp/+}$ and *Vangl2*$^{Lp/Lp}$ organs, as in wild-type littermate metanephroi, condensing renal mesenchyme was visualized around ureteric bud branch tips, and adjacent nephron vesicles were apparent (Fig. 2D–F). Despite the smaller size of E14.5 organs, both proliferation and apoptosis measured *in situ* across the whole metanephros was similar in wild-type and *Vangl2*$^{Lp/Lp}$ organs (Fig. 2G–P). By E18.5, the wild-type metanephros had undergone further growth and acquired its characteristic ‘kidney bean shape’, and its centre was occupied by a slit-like renal pelvis, the cavity which receives urine from the collecting duct system (Fig. 3A). Overall histology of E18.5 *Vangl2*$^{Lp/+}$ kidneys (Fig. 3B) appeared similar to their wild-type counterparts, whereas *Vangl2*$^{Lp/Lp}$ E18.5 kidneys lacked the normal curved profile and contained a renal pelvis which resembled a hole rather than the normal

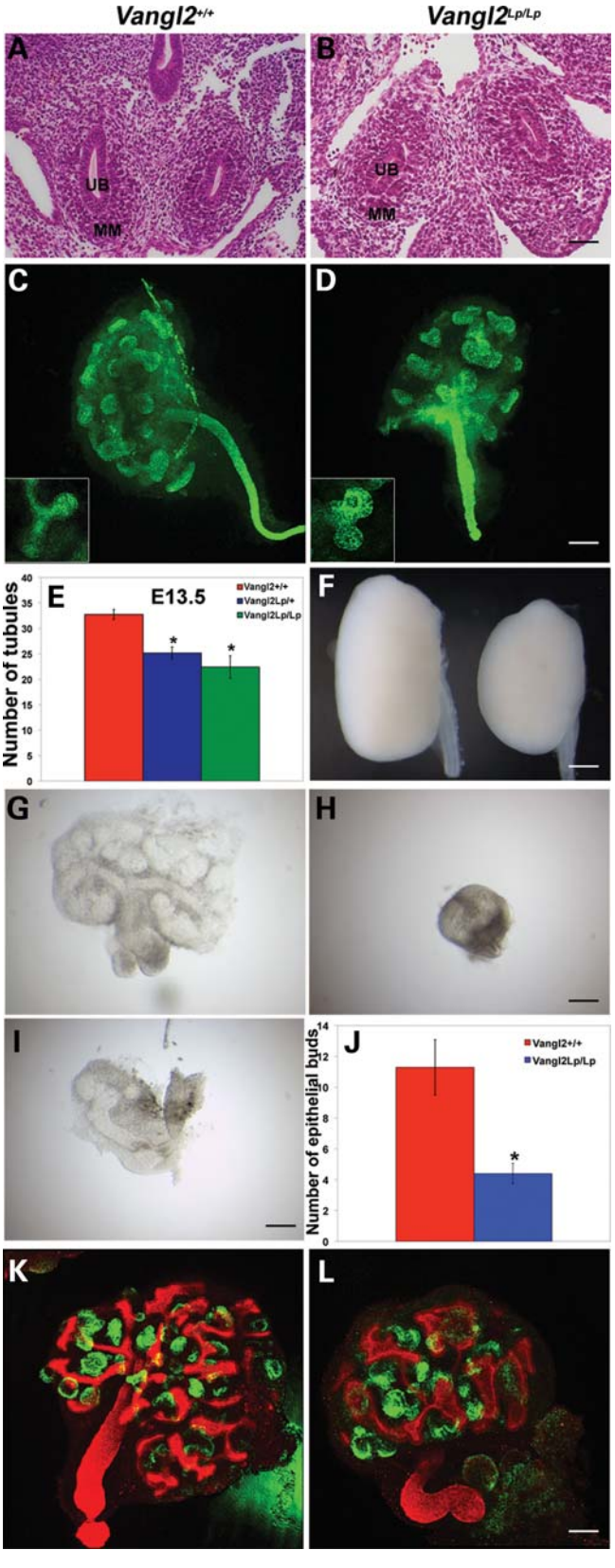

elongated cavity (compare the outline of the organ in Fig. 3C with A). At this stage, the wild-type kidney contained a well-demarcated cortex and medulla (Fig. 3D). The outer cortex comprised ureteric bud branch tips whereas the cortex below this contained S-shaped bodies, which are immature nephrons beginning to segment into glomerular and proximal tubule epithelia (Fig. 4A–D), as well as proximal tubules and glomeruli (Figs 3D, G, 4E and F). The demarcation between the cortex and medulla was unclear in *Vangl2*$^{Lp/Lp}$ organs (Fig. 3F), with heterozygous kidneys (Fig. 3E) having an intermediate appearance between null mutant and wild-type littermates. Whereas proximal tubules and glomeruli appeared grossly normal in *Vangl2*$^{Lp/+}$ organs (compare Fig. 3H with G), homozygous mutant kidneys contained subsets of glomeruli which were small or distorted (a feature examined in detail below) and some tubules contained attenuated brush borders as visualized by periodic-acidSchiff (PAS) staining (Fig. 3I). The brush border of a differentiated proximal tubule cell comprises microvilli inserting into the apical zone of the epithelium, and both zones are rich in actin (25). Using phalloidin staining to visualize the f-actin cytoskeleton, some proximal tubule profiles in E18.5 *Vangl2*$^{Lp/Lp}$ kidneys had an irregular and discontinuous actin pattern versus proximal tubules in wild-type littermates (compare Fig. 3K with J). Although some tubules in fetal null mutant kidneys appeared dilated (Fig. 3I), an overt polycystic phenotype was not seen.

Several PCP molecules are expressed in the nephrogenic cortex and in differentiating podocytes

Vangl2 protein has previously been immunodetected in developing murine kidneys in ureteric bud branch tips, collecting ducts, nephron vesicles and forming glomeruli (S-shaped bodies and podocyte epithelia) (7,27). Because the results of

Figure 1. Early branching morphogenesis is disrupted in *Vangl2*^{Lp} kidneys *in vivo* and *in vitro*. Haematoxylin- and eosin-stained transverse sections through whole E11.5 embryos showed similar appearances in both wild-type (**A**) and *Vangl2*$^{Lp/Lp}$ (**B**) littermate embryos ($n = 3$ each genotype). Both had paired metanephric rudiments in which the ureteric bud (UB) penetrated into metanephric mesenchyme (MM). E13.5 whole z-stack images of wild-type (**C**) and *Vangl2*$^{Lp/Lp}$ (**D**) kidneys immunostained for cytokeratin (green signal). Inserts in (C) and (D) show representative zoomed-in images of typical ureteric bud tips; *Vangl2*$^{Lp/Lp}$ bud tips are frequently shorter and broader than in wild-type. (**E**) There was a significant ($P < 0.01$) reduction in numbers of ureteric bud branch tips in *Vangl2*^{Lp} heterozygote ($n = 12$) and homozygote ($n = 5$) versus wild-type ($n = 4$) metanephroi. At E18.5, *Vangl2*^{Lp} kidneys (**F,** right) appeared smaller and abnormally shaped in comparison to wild-type littermates (F, left). After 2days in culture, E11.5 mutant explants (**H** and **I**) appeared variably growth-retarded versus wild-type organs (**G**). Furthermore, these cultured *Vangl2*$^{Lp/Lp}$ metanephroi ($n = 10$) had significantly ($P = 0.009$) fewer bud tips in comparison to wild-type littermates ($n = 7$) (**J**). (**K** and **L**) To assess potential further differentiation *in vitro*, E12.0 metanephroi were cultured for 5 days and then immunostained for both cytokeratin (red) to highlight the arborizing ureteric tree, and WT1 (green) to highlight podocytes within glomeruli. After 5 days, wild-type explants (K; $n = 3$) appeared consistently larger than the *Vangl2*$^{Lp/Lp}$ organ (L; $n = 3$). The ureteric tree in mutants appeared distorted with wider branch tips. Balls of WT-1-expressing cells, primitive glomeruli, formed in both genotypes. Scale bars: (A and B) 50 μM, (C and D) 125 μM, (F) 62.5 μM, (G–I) 63 μM and (K and L) 125 μM.

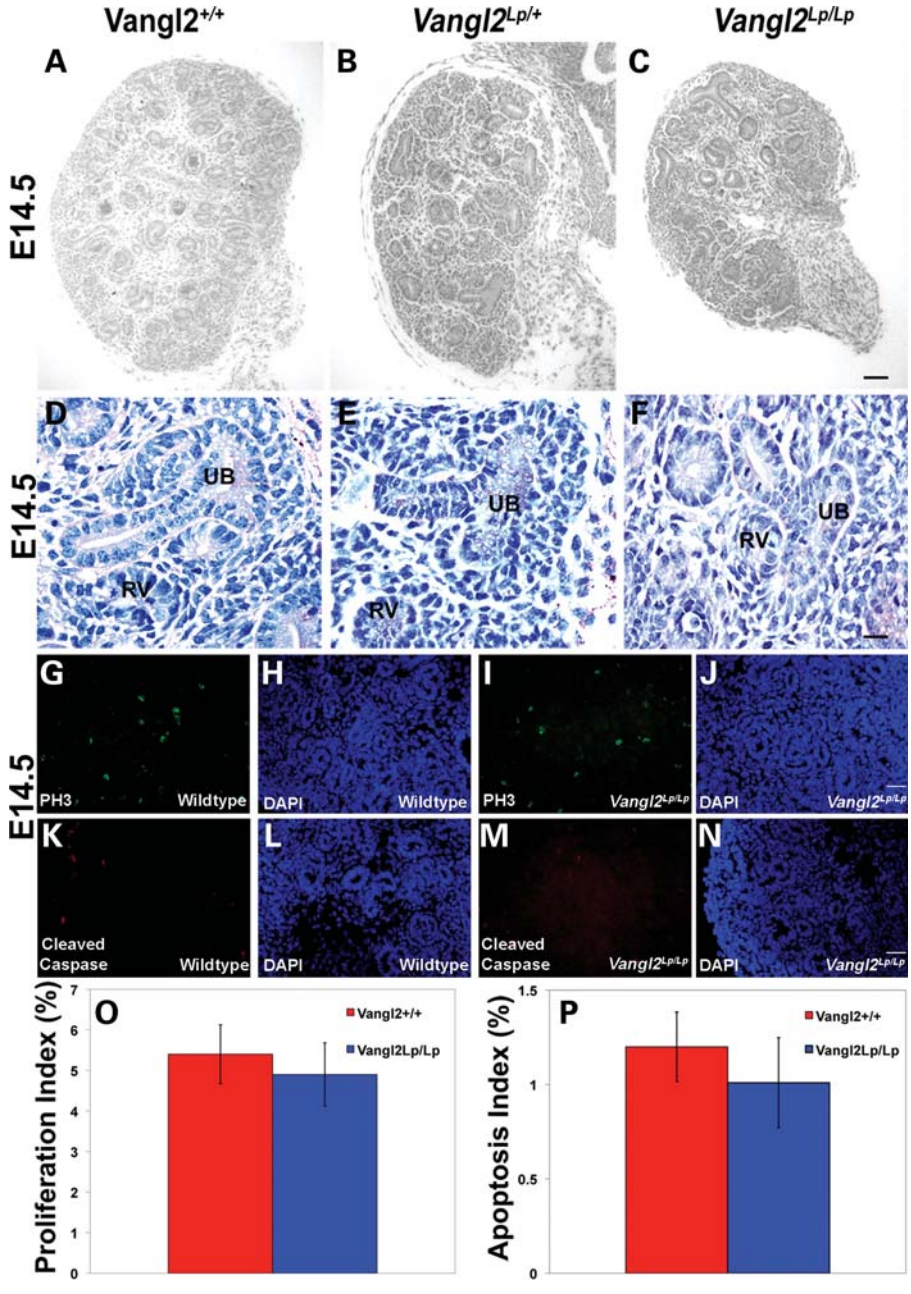

Figure 2. E14.5 *Loop-tail* kidneys exhibit normal histology and no change in proliferation or apoptosis. Haematoxylin-stained sections of E14.5 wild-type (**A** and **D**), *Vangl2*$^{Lp/+}$ (**B** and **E**) and *Vangl2*$^{Lp/Lp}$ (**C** and **F**) metanephroi. At E14.5, although all three genotypes contained renal vesicles (RV) and ureteric bud branches (UB), *Vangl2*$^{Lp/Lp}$ organs appeared smaller than wild-type littermates (compare C with A). Analysis of the percentage of proliferating cells in E14.5 whole kidney sections by immunostaining with anti-pH3 (**G, I** and **O**) or of apoptosis with anti-cleaved caspase 3 (CC3) (**K, M** and **P**) and DAPI **(H, J, L** and **N)** revealed no significant differences between wild-type (red) and *Vangl2*$^{Lp/Lp}$ (blue). Proliferation and apoptotic indices were, respectively, calculated by counting the numbers of phosphor histone-H3 (*PH3*)- or cleaved caspase 3 (*Cleaved Caspase*)-expressing cells in kidney sections from three individuals of each genotype, and showing them as a percentage of total (DAPI-stained) nuclei. Images are representative of at least three animals in each category. Scale bars: (A–C) = 100 μM and (D–F) = 25 μM.

those studies are clear, we did not attempt to replicate them here. Instead, to gain a greater understanding of PCP pathway components in kidney development, we examined the distribution of Scribble 1 (Scrib), a protein mutated in the *Circletail* mouse (34), and Celsr1, a molecule known to be critical for lung branching (26). In wild-type E18.5 kidneys, which contain a spectrum of differentiating structures, Scrib was immunodetected (Fig. 4A, C and E) most prominently in the outer (nephrogenic) cortex where ureteric bud branch tips, mesenchymal condensates, vesicles and S-shaped bodies expressed the protein. Maturing podocytes were also positive. Celsr1 (Fig. 4B, D and F) was expressed in the cortex of the E18.5 kidney where it was most prominent in more mature components such as collecting duct stalks and S-shaped bodies (Fig. 4D) rather than bud tips and vesicles. Celsr1 was also detected in podocytes and adjacent proximal

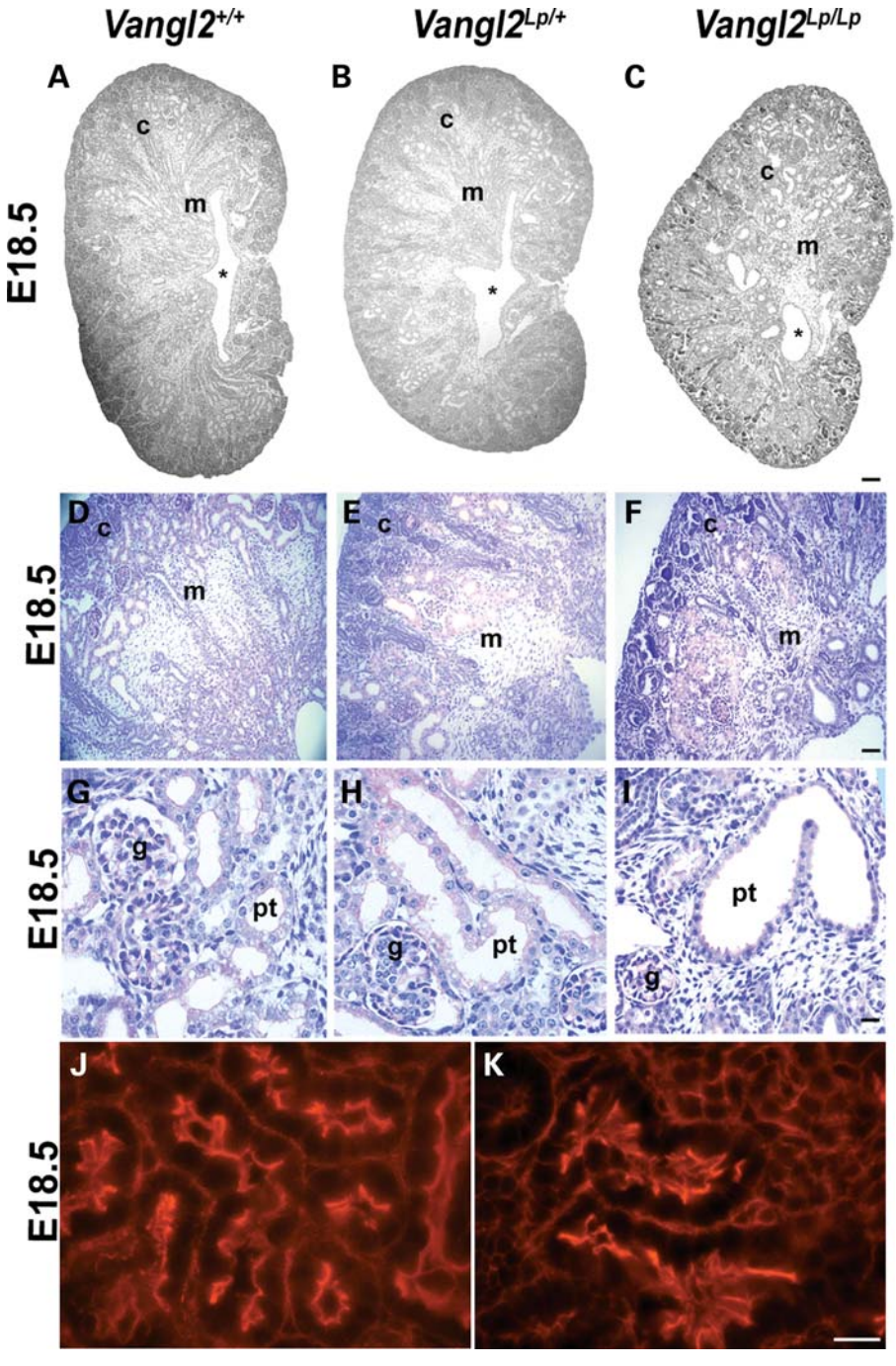

Figure 3. Histology of E18.5 kidneys. E18.5 (**A–K**) kidneys from wild-type (A, D, G and J), *Vangl2*$^{Lp/+}$ (B, E and H) and *Vangl2*$^{Lp/Lp}$ (C, F, I and K) mice. At E18.5, homozygous (C) kidneys appeared smaller than wild-type littermate kidneys (A). *Vangl2*$^{Lp/Lp}$ kidneys are visibly misshaped, with a hypoplastic medulla (compare F with D) and the renal pelvis (*) lacks the normal slit-like shape seen in wild-type and *Vangl2*$^{Lp/+}$ kidneys (compare C with A and B). Occasional enlarged and distorted proximal tubules with attenuated brush borders (pink) were observed in *Vangl2*$^{Lp/Lp}$ mice (I), but there was no overt cystic phenotype. Phalloidin staining highlights disruption to the organization of the actin cytoskeleton in *Vangl2*$^{Lp/Lp}$ proximal tubules; particularly at the apical surface (K), in comparison to the ordered cytoskeletal arrangement in *Vangl2*$^{+/+}$(J). Images are representative of at least three animals in each category. *c*, cortex; *g*, glomerulus; *m*, medulla; *pt*, proximal tubule. Scale bars: (A–C) = 200 μM, (D–I) = 25 μM and (J and K) = 5 μM.

tubules (Fig. 4F). No significant signal was obtained when primary antibodies were omitted (Fig. 4G and H). Previous studies have established the specificity of these antibodies by attenuation and/or mislocalization of the Vangl2 protein in *Lp/Lp* embryos and the Celsr1 protein in *Crsh/Crsh* embryos (26,35,36). Finally, we used an established *in vitro* cell culture system (37) to seek the expression of a panel of PCP genes in both undifferentiated and differentiated mouse podocytes (Fig. 5). The *in vitro* differentiation is characterized by a change from proliferating cells with few processes, to quiescent

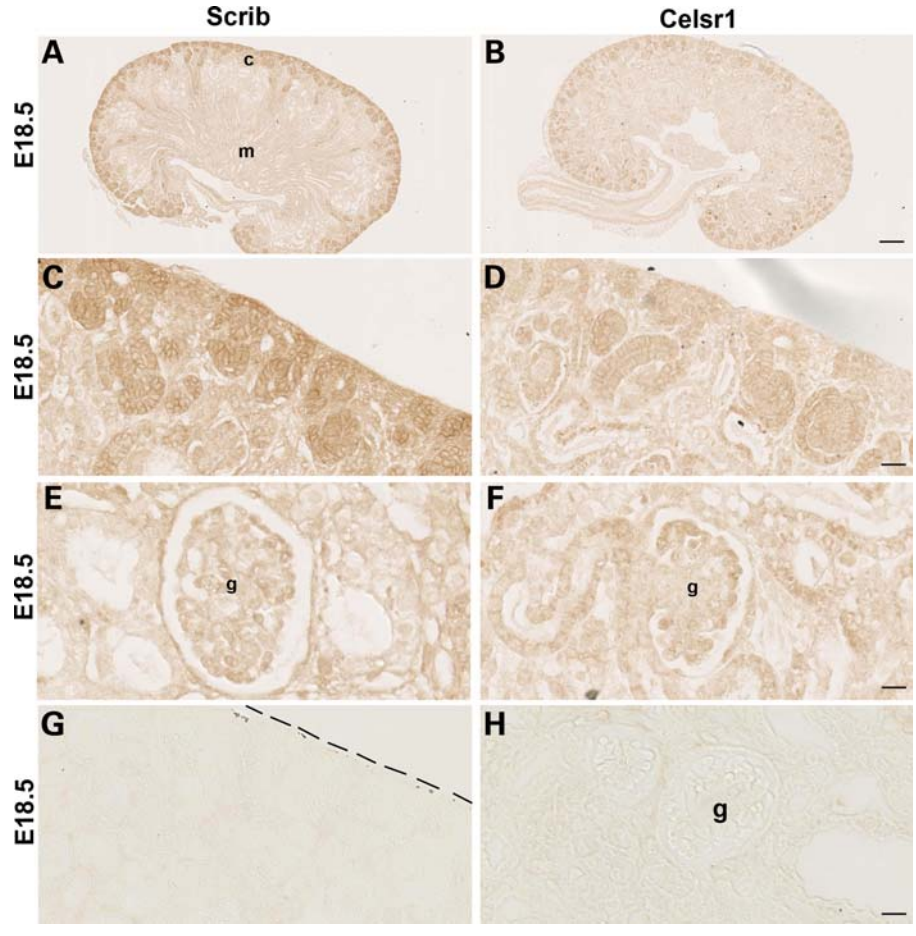

Figure 4. PCP pathway components are expressed in E18.5 kidney. Immunostaining (brown) for Scrib (**A, C** and **E**) and Celsr1 (**B, D** and **F**) in E18.5 sections (note there is no counterstain in these sections). Scrib expression was prominent in the outer (nephrogenic) cortex (*c* in A) where it was found in diverse structures such as ureteric bud tips, mesenchymal condensates and vesicles (C). Scrib was also expressed in maturing podocytes located in the periphery of the glomerular tuft (E). Celsr1 expression was noted in collecting duct stalks and S-shaped bodies just below the nephrogenic zone (B and D). Expression of Celsr1 was also observed in proximal tubule and podocyte epithelia (F). Where primary antibodies were omitted, no significant staining was observed (**G** and **H**). Dashed line in (G) marks edge of kidney; below line is tissue. *c*, cortex; *g*, glomerulus; *m*, medulla; pt, proximal tubule. Scale bars: (A and B) 100 μM, (C and D), (G) 25 μM and (E, F and H) 12.5 μM.

cells with up to several actin-rich processes which grow from the cell body (Fig. 5A and B). In both conditions (Fig. 5C and D), podocytes expressed *Vangl2* and well as *Vangl1*, *Celsr1*, *Fat4*, *mouse prickle1* and *mouse prickle2 (mpk1 and mpk2*; 38,39).

E18.5 *Vangl2$^{Lp/Lp}$* kidneys show abnormalities of glomerular maturation

The above observations prompted us to look closely at forming glomeruli in E18.5 kidneys. We conducted a careful analysis of glomerular morphology undertaken by an observer, blinded as to the genotypes of the organs, who assigned at least several tens of glomeruli in each kidney into one of four categories, according to the extent of maturation or morphological disruption, with 'a' being the most mature and 'd' being the most abnormal (Fig. 6A). In wild-type kidneys, over 95% of glomerular cross-sections displayed two or more capillary lumens (a marker of maturity), and most had more than two such lumens (Fig. 6B). By contrast, in late-gestation *Vangl2$^{Lp/Lp}$* kidneys, <90% of all glomeruli contained two or more capillary lumens and, more strikingly, only half of these had more than two lumens. Moreover, in the null mutant kidneys, a small subset of glomeruli were malformed, with a distorted glomerular tuft (subtype d); such profiles were never observed in several hundreds of glomeruli scored in wild-type kidneys. The average diameter of *Vangl2$^{Lp/Lp}$* glomerular tufts (i.e. the central ball of cells without the surrounding Bowman's space and outer parietal epithelium) was significantly less than in wild-type kidneys (Fig. 6C). For *Vangl2$^{Lp/+}$* kidneys, values were intermediate between wild-types and null mutants (Fig. 6B and C). We also sought proliferating cells in glomerular tufts by an immunohistochemical method (Fig. 6D) and found that the proportion of positive nuclei was significantly reduced in *Vangl2$^{Lp/Lp}$* glomeruli versus either wild-type or *Vangl2$^{Lp/+}$* kidneys (Fig. 6E). When comparing the most mature-looking glomeruli (i.e. subtype 'a.') in the three genotypes, immunostaining patterns for both synaptopodin, a molecule which regulates podocyte actin dynamics (40), and nephrin, a component of the junctions between podocyte foot processes (24),

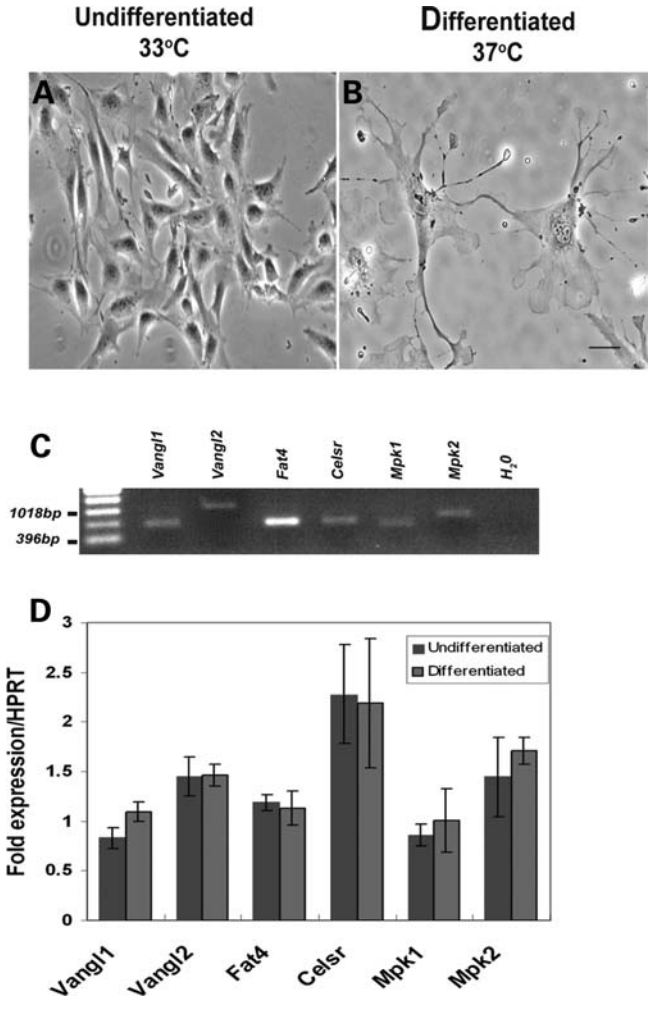

Figure 5. RT–PCR expression of PCP pathway components in mouse podocytes. Phase-contrast micrographs of undifferentiated (**A**) and differentiated podocytes (**B**) showing the extensive process formation characteristic of the *in vivo* podocyte phenotype. *Vangl1/2*, *Fat4*, *Celsr1* and *Mpk1/2* transcripts were identified in undifferentiated podocytes (**C**) but no statistically significant ($P < 0.05$) differences in expression between undifferentiated and differentiated cells were identified by quantitative real-time PCR (**D**). Results from three independent experiments are shown. Scale bar, 25 μM.

appeared similar (Fig. 6D). As assessed by phalloidin staining, the crenellated pattern of f-actin evident in wild-type glomerular tufts, probably representing actin in both the basal zone of podocytes and in closely adjacent endothelia in forming capillary tufts (41), appeared less prominent in *Vangl2*$^{Lp/Lp}$ glomeruli (Fig. 6F).

Gene expression in E18.5 kidneys

To assess whether the various morphological aberrations described above in E18.5 *Vangl2*$^{Lp/Lp}$ kidneys corresponded to transcriptional changes, levels of transcripts were measured by quantitative PCR (32) in RNA extracted from whole organs. The genes analysed (Supplementary Material, Table S1) included those coding for: (i) transcription factors, growth factors/receptors and adhesion molecules implicated in metanephric-branching morphogenesis and nephron formation; (ii) proteins characteristically expressed by specific differentiated epithelia within collecting ducts, glomeruli, proximal tubules and loops of Henle; and (iii) ciliary/basal body proteins, mutations of which cause polycystic kidney disorders. Comparing levels of these mRNAs factored for levels of housekeeping transcripts between wild-type and *Vangl2*$^{Lp/Lp}$ organs, none were significantly different (i.e. $P < 0.05$; data not shown). This analysis did, however, suggest that levels of four genes (*Shh*, *Patched 1*, *Fgf7* and *Ift88*) tended to differ between the two genotypes. We therefore re-examined levels of these transcripts using an independent set of qPCR assays on cDNA from additional embryos. The results of these assays (Supplementary Material, Fig. S1) failed to confirm the previously observed trends.

Postnatal *Vangl2*$^{Lp/+}$ kidneys have a modest reduction in glomerular numbers

As depicted in Figure 7 and data not shown, *Vangl2*$^{Lp/+}$ kidneys of 1-month-old mice were found to have a modest but significant deficit in glomerular numbers, although immunostaining for synaptopodin and nephrin was normal, and there was no sign of glomerulosclerosis (scarring) as assessed by PAS staining (Fig. 7). Tubules showed no cyst formation. Finally, we found no difference in urinary albumin (Fig. 7H) or retinol-binding protein excretion (Fig. 7I) between 12-week-old wild-type and *Vangl2*$^{Lp/+}$ mice. An increased level of albumin would be expected if there existed significant impairment of the glomerular permeability barrier (i.e. a podocyte function). An increased level of retinol binding protein would be expected if proximal tubule uptake of small molecules had been impaired.

DISCUSSION

PCP genes and kidney development

In the fetal kidney, the PCP pathway is considered to set a limit on the diameter of differentiating tubules because *Wnt9b* mutation causes cystic kidneys, perturbing the normal CE-like rearrangement of existing epithelial cells during tubule elongation and narrowing (42). Later in mouse kidney maturation, tubule diameter is limited by a predominance of polarized cell divisions aligned along the longitudinal axis of the tubule (43). This, in turn, requires the function of primary cilia (43), organelles which protrude from the apical epithelial surface and which transduce signals triggered by tubular fluid flow and perhaps also by yet-to-be defined components in the fluid (44). Oriented cell divisions and tubule elongation are disrupted by mutation of *Fat4*, a PCP gene, the protein product of which is also detected in primary cilia (44,45). Intriguingly, the cystic kidney phenotype observed in *Fat4* mutants is accentuated when mice are additionally haploinsufficient for *Vangl2* (45). Another link between renal cysts, PCP and ciliary sensing is provided by inversin, a protein mediating a switch from canonical to non-canonical Wnt signalling (46). Expression of inversin is upregulated by fluid flow, and *Invs* mutations lead to cystic kidneys (46).

In our current study, we failed to find a cystic phenotype either in *Vangl2*$^{Lp/Lp}$ and *Vangl2*$^{Lp/+}$ fetal kidneys or in

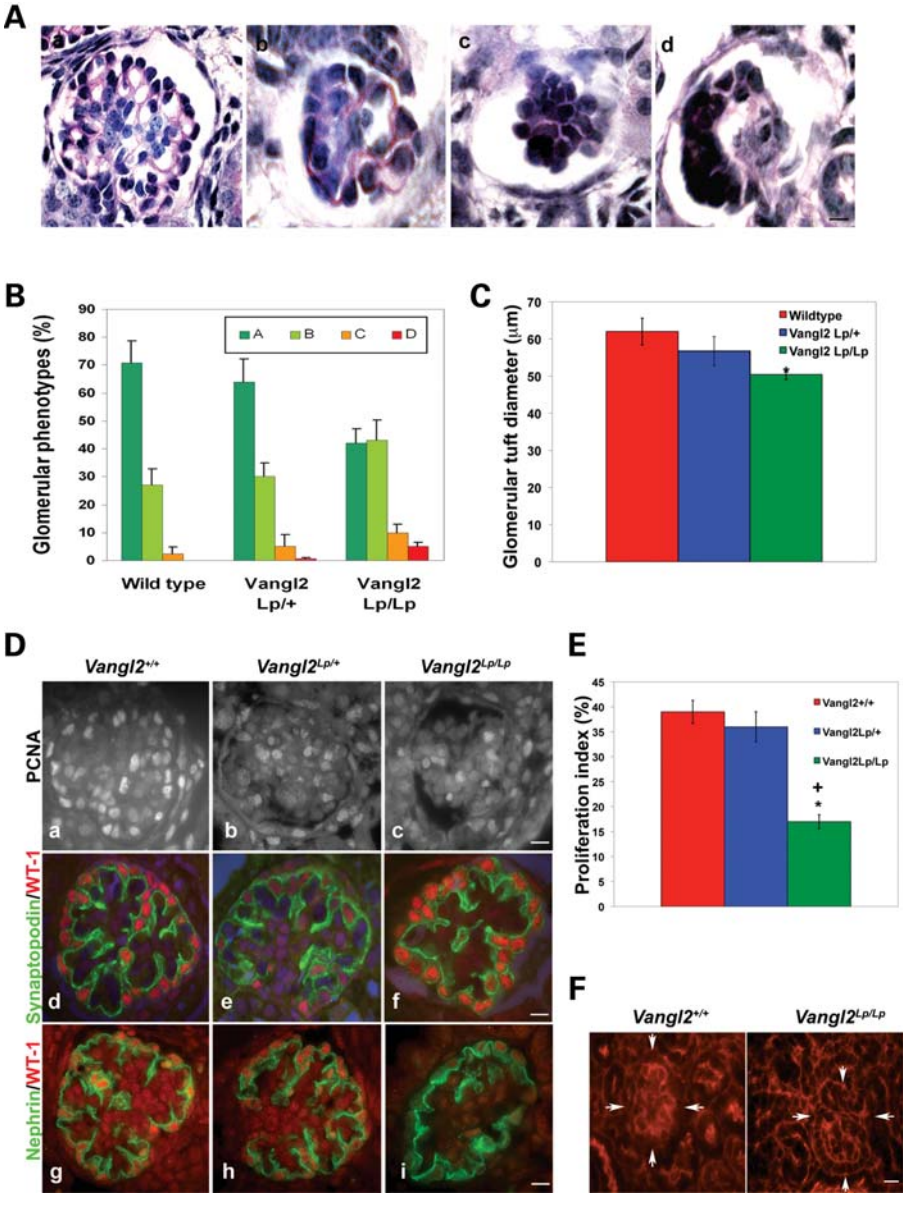

Figure 6. Disruption of *Vangl2* causes glomerular maturation defects. All data in this figure are from E18.5 kidneys. Glomerular tuft morphology was assessed according to the following categories: a, more than two capillary lumens per tuft; b, one or two capillary lumens; c, no capillary lumens; d, abnormal and disrupted glomerular tuft. (**A**) Representative glomeruli in each category. (**B**) Proportions of glomeruli in the three genotypes ($n = 3$–4 kidneys in each set). The commonest phenotype of wild-type and heterozygous glomeruli was category a. *Vangl2*$^{Lp/Lp}$ glomeruli showed a shift of phenotypes such that glomerular types a and b were equally common and they contained a small subset of category d never seen in wild-type kidneys. *Vangl2*$^{Lp/Lp}$ glomerular tufts had a significantly reduced glomerular diameter (**C**). (**D**a–c) Proliferation of glomerular cells as assessed by immunodetection of PCNA (white nuclei). A reduction in the frequency of proliferation in homozygous organs was confirmed upon counting proportions of proliferating cells in the glomerular tuft (**E**). (Dd–f). Synaptopodin (green) and WT-1 (red) co-staining showed similar appearances in the three genotypes when mature glomeruli were assessed. (Dg–i) Nephrin (green) immunostaining showed similar appearances in the three genotypes when mature glomeruli were assessed. (**F**) Phalloidin staining highlighted the typical crenellated pattern of f-actin in *Vangl2*$^{+/+}$ glomerulus (arrowed on the left frame) which appeared less apparent in a *Vangl2*$^{Lp/Lp}$ glomerulus (arrowed on the right frame). Counts were performed on at least 20 glomeruli from at least three to four separate kidneys in each genotype. $^{*}P < 0.05$ compared with wild-type; $+P < 0.05$ compared with heterozygotes. Scale bars = 15 μM.

1-month-old *Vangl2* heterozygous kidneys. It remains possible, however, that the absence of *Vangl2* might lead to cysts in the weeks after birth and that *Vangl2* haploinsufficiency might cause kidney cysts later in adulthood. As assessed by PCR of late-gestation kidneys, the *Vangl2*$^{Lp/Lp}$ mutation did not significantly alter the expression of numerous transcripts (e.g. *Bbs1/4*, *Ift88*, *Invs*, *Mks1*, *Ofd1* and *Pkd1/2*), which encode ciliary proteins implicated in genetic cystic kidney diseases. Furthermore, we found that tubules in *Vangl2*$^{Lp/Lp}$ fetal kidneys did contain primary cilia (data not shown), as assessed by immunostaining for acetylated α-tubulin and IFT88 (19,47), although their orientation or numbers were not formally assessed.

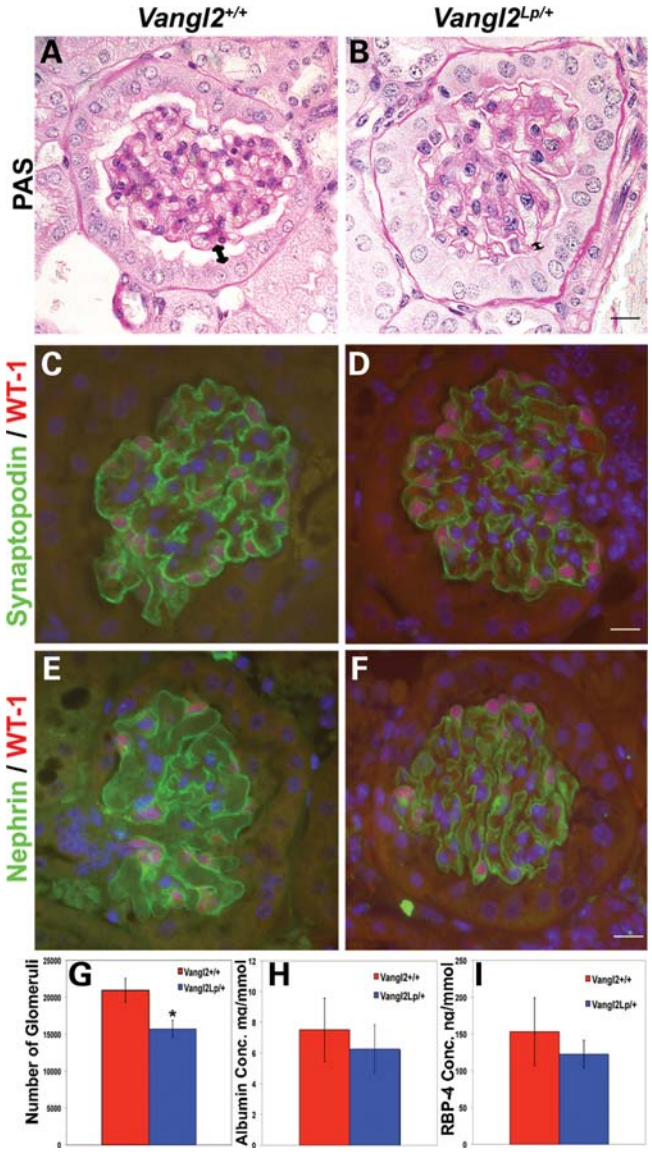

Figure 7. Histology of adult *Vangl2*$^{Lp/+}$ kidneys. (**A** and **B**) PAS staining of 4-week-old *Vangl2*$^{Lp/+}$ mice kidneys show a normal appearance with no scarring. Expression patterns of synaptopodin (green in **C** and **D**) and nephrin (green in **E** and **F**) were similar in wild-type and heterozygous glomeruli. (**G**) Reduced glomerular numbers per kidney in *Vangl2*$^{Lp/+}$ mice ($n = 4$) versus wild-type littermates ($n = 4$). No significant differences in the ratio of urinary albumin/creatinine (**H**) or retinol-binding protein (RBP)/creatinine (**I**) were found between *Vangl2*$^{Lp/+}$ and *Vangl2*$^{+/+}$ mice. Scale bars = 15 μM.

Despite the above insights into tubule diameter regulation, the roles, if any, of the PCP pathway on other metanephric processes, such as initiation of the kidney, ureter formation, branching morphogenesis and glomerular morphogenesis, have been unclear. We found that, at least in the C3H/HeH background studied, Vangl2 deficiency did not prevent ureteric bud formation nor aggregation of intermediate mesodermal cells, which together comprise the metanephric rudiment. Nor did Vangl2 deficiency lead to ureteric duplication or ureter dilatation, the latter structure derived from the distal part of the ureteric bud.

Vangl2 is required for kidney-branching morphogenesis

Our data show that *Vangl2* mutation strikingly impairs the arborization of the ureteric tree and that it is also associated with impaired glomerular maturation. This is the first demonstration that a core PCP component is required for normal development of both ureteric bud and metanephric mesenchyme-derived structures. The fact that developing epithelia in both lineages express Vangl2 protein is consistent with intrinsic functions in ureteric bud branches and nascent glomeruli (7, 27). Compared with time-matched wild-type organs, the growth restriction observed in explanted *Vangl2* null mutant E11.5 rudiments appeared more prominent than that seen in either E12.0 explants or *Vangl2* null mutant metanephroi *in vivo*. One possible explanation is that the serum-free tissue culture conditions used for such experiments may be more 'stressful' for younger rudiments and that any additional insult (in this case the *Vangl2* mutation) results in a more severe *in vitro* phenotype.

Our immunohistochemistry studies which localized the PCP proteins Scrib and Celsr1 in diverse structures in the still-developing outer cortex of the late-gestation kidney concur with patterns of transcripts as reported in the Genito-Urinary Development Molecular Anatomy Project database [GUDMAP (48)]. We suggest that the branching impairment found in both *Vangl2*^{Lp} heterozygous and homozygous metanephroi is an intrinsic defect operating within ureteric bud epithelia. In a quantitative PCR survey, we found no significant differences in levels of transcripts for growth factor signalling molecules (e.g. *Areg*, *Bmp4*, *Egf, Fgf7*, *Hgf*, *Gdnf*, *Tfga* and *Wnt11*) which are known to regulate kidney branching (21). Instead, there are probably mechanistic parallels between the defective branching we observed in *Vangl2*^{Lp} *embryonic* kidneys and the defects in lung branching reported by Yates *et al*. (26) in *Vangl2* mutant mice. This study showed that branching defects were due to impaired tissue morphogenesis as a result of cytoskeletal disruption. In fact, the lung-branching defect in these mutants could not be rescued *in vitro* upon the addition of Fgf10, a growth factor that normally induces lung branching (26).

More likely, Vangl2 mediates branching in both the lung and kidney in a cell-autonomous manner acting, as it does in neural tube closure (11), through ROCK-mediated cytoskeletal actions. ROCK indirectly inhibits actin filament depolymerization (49), and when perturbed, over time, actin monomers that are required to continue actin polymerization for migration and cell movement become limited. Indeed, the branching defects observed in *Vangl2*$^{Lp/Lp}$ lungs can be modelled by chemical inhibition of this enzyme in organ culture of wild-type embryonic lungs (26), and it is already established that branching morphogenesis in the metanephros is sensitive to ROCK activity (50–52). While we did not detect any marked alteration in pattern of f-actin in *Vangl2*$^{Lp/Lp}$ ureteric bud branch tips (data not shown), it was notable that the apical f-actin pattern appeared irregular in mutant proximal-like tubules. Future studies should use conditional deletion *Cre-LoxP* strategies, for example using the ureteric lineage-specific *HoxB7/Cre* line (53), to confirm the hypothesis that the kidney-branching defect is caused by deficiency of Vangl2 within arborizing epithelia.

The retardation of metanephric-branching morphogenesis which we measured in the first days of *Vangl2*$^{Lp/Lp}$ metanephric development likely explains why the late-gestation null-mutant kidney has a poorly developed medulla and renal pelvis because bud-derived collecting ducts normally populate the medulla and contribute to the shape of the pelvis. As assessed by qPCR, there were no differences between null mutant and wild-type late-gestation kidneys in expression of differentiation markers of specific tubule epithelia (e.g. *Ggt1* for proximal tubules, *Umod* for loops of Henle and *Aqp2* for collecting ducts). These observations are consistent with the idea that Vangl2 is not required for terminal differentiation of tubules but instead modulates their morphogenesis.

Humans with NTDs sometimes also have kidney malformations

Historically, individuals born with NTDs often died from renal failure, which was perceived as arising from excessive back-pressure on the kidneys from impaired urine flow combined with bacterial infection ascending from urine pooled in poor-emptying urinary bladders. Some individuals with NTDs, however, are born with kidney malformations such as agenesis (unilateral absent kidney), gross defects in renal shape (horse-shoe kidney) and ureteric duplication (duplex kidneys) (28–30). These historical clinical observations are consistent with the idea that both the renal malformation and NTD arise from common, perhaps genetic or environmental, causes. On the basis of our observations in mice, we suggest that the subset of individuals with NTDs who also have kidney malformations may be found to have *VANGL* or other PCP gene mutations.

Vangl2 is required for kidney glomerular maturation

We also found that the tufts of glomeruli in *Vangl2*$^{Lp/Lp}$ late-gestation kidneys were smaller than their wild-type littermates. This was associated with a decrease in percentage of proliferating cells within the tufts. Glomerular tufts initially comprise only differentiating podocytes and they then become invaded by blood capillary loops and pericyte-like mesangial cells (23,54). Our methodology could not distinguish whether the proliferation defect in *Vangl2*$^{Lp/Lp}$ tufts affected a specific type of cell although proliferation did appear to be reduced in the periphery of the tuft (compare null mutant with wild-type in Fig. 6D) where podocytes are found. The cause of the proliferation defect is uncertain, but we note that Vangl2 has been implicated in the expansion of muscle (4) and neural (3) stem cells. In the latter example (3), late-gestation *Vangl2*$^{Lp/Lp}$ brains showed a significant reduction in dividing progenitors even though earlier in gestation, exactly as found in E14.5 *Vangl2* mutant metanephroi, the numbers of proliferating cells were the same as in controls. Thus, we speculate that Vangl2 may regulate the numbers of glomerular precursor cells within the primitive nephron. Consistent with this interpretation of the *Vangl2*$^{Lp/Lp}$ glomerular tuft size in relation to podocyte proliferation, we found that isolated differentiating podocytes express an array of PCP transcripts, including *Vangl2*.

Podocytes are extremely plastic cells and as such they are able to alter their shape via molecular regulation of their intracellular cytoskeleton. Cytoskeletal disruption caused by injury or genetic disorders of glomerular function leads to misshaping or absence of foot processes (24,55). Unless this process can be reversed, it results in leakage of protein into the glomerular filtrate, glomerular scarring and eventually, chronic renal failure. Therefore, an understanding of the molecular mechanisms regulating podocyte architecture is likely to prove valuable for treatment of glomerular dysfunction. Synaptopodin plays an essential role in the regulation of podocyte actin dynamics and RhoA is a target of the molecule (40). However, we noted no overt abnormality in the pattern of synaptopodin protein in *Vangl2* mutant glomeruli. In a recent cell culture study, Babayeva *et al*. (27) reported that siRNA depletion of podocyte Vangl2 reduced the number of cell projections, decreased actin stress fibres and impaired cell motility. How this result relates to the glomerular phenotype we observed in *Vangl2*$^{Lp/Lp}$ kidneys is not clear although it provides proof of principle that Vangl2 plays an active role in podocyte biology. Ichimura *et al*. (56) recently reported that immature podocytes express primary cilia *in vivo* but that these organelles are lost with full differentiation. In future, it would be interesting to determine whether the Vangl2 protein can be found associated with these structures.

We note that endothelia in developing glomeruli have been reported to express *Vangl2* transcripts (48) and, if capillary migration were to be compromised, this may help explain why *Vangl2*$^{Lp/Lp}$ tufts have a deficit in capillary lumens. The apparent attenuation of f-actin we observed in mutant fetal glomeruli may represent a combined aberration in the cytoskeleton of both podocytes and closely adjacent endothelia (41). According to our current data and those from GUDMAP (48), podocytes also express *Vangl1* transcripts. Given the fact that, in other tissues, there is genetic interaction between *Vangl1* and *Vangl2* (12), we predict that double mutants would have a much more severe glomerular phenotype than that displayed by *Vangl2* mutants in the current study. Finally, we note that upregulation of canonical Wnt/β-catenin signalling has been implicated in the pathophysiology of acquired proteinuric glomerular diseases (57). In future, a definitive exploration of the roles of Wnt canonical and non-canonical/PCP pathways in glomeruli genes will require their selective deletion in these cells at different stages of glomerular differentiation using *Cre-LoxP* technology (58).

Vangl2 and nephron numbers

In mice, new nephrons continue to be generated during the first week after birth (22,59). Non-viability of homozygous *Vangl2* mice due to severe NTDs precluded analyses of their kidneys beyond the fetal period. Instead, we analysed kidneys of *Vangl2*$^{Lp/+}$ mice 4 weeks after birth. These animals are overtly healthy although they have a deformity consistent with their name, *Looptail*. Our data show that haploinsufficiency of *Vangl2* results in a modestly decreased nephron number. Our method for quantifying glomerular numbers relied on acid-mediated dissociation of the kidney (60). While it is possible this method may be less accurate

than stereology (61,62), any directional bias would be equal in wild-type and *Vangl2*$^{Lp/+}$ samples because the latter displayed no tissue abnormalities such as cyst formation which might affect the efficiency of dissociation. Because we demonstrated that *Vangl2*$^{Lp/+}$ as well as homozygous *Vangl2* mice have a branching defect, the reduction in final glomerular numbers may be caused by a relative lack of branch tips available to induce mesenchymal cells to differentiate into nephrons.

It is striking that human populations contain otherwise healthy individuals with a very wide range of glomerular numbers (~1–2 million) per kidney (62). On the basis of the results of animal experiments (60,61) and human studies (63), it is likely that both environmental influences (e.g. the diet a mother eats when pregnant) and genetic factors (e.g. polymorphisms of genes expressed in the developing kidney) together determine nephron number in an individual. Moreover, people with essential hypertension probably have a congenital nephron deficit (62) and animals born with too few nephrons are prone to arterial hypertension later in life (61). Further studies will be required to determine whether *Looptail* mice are prone to hypertension or susceptible to glomerular scarring as they age. However, we suggest that mutation or variants of *VANGL* and other PCP genes should be considered as possible causes of the variable glomerular numbers observed in human kidneys.

MATERIALS AND METHODS

All reagents were obtained from Sigma Chemical (Poole, UK) unless otherwise stated.

Histology and immunostaining

The Looptail mice (Jackson Laboratories, Bar Harbour, USA) contain a point mutation which causes a serine to asparagine transition at position 464 resulting in loss of *Vangl2* function (10,64). Mice were maintained on a C3H/HeH background. *Vangl2*^{Lp} homozygotes and heterozygotes were identified by craniorachischisis and looped-tail phenotypes, respectively, or genotyped using a pyrosequencing assay to amplify the mutation directly (forward: 5′Biotin GTCCTGGCGCTTCAA GAGGA; reverse: NNNGGCCAAACAGTGGACCTTGG; sequence: CAGTGGACCTTGGTGA); wild-type littermates were used as controls. Kidneys were fixed in 4% paraformaldehyde, dehydrated, wax-embedded and sectioned at 5 μm. For some antibodies, 10 μm cryosections were used. In some experiments, the following stains were used: PAS to visualize all basement membranes and also proximal tubule brush borders; haematoxylin to visualize nuclei; and eosin to define cytoplasm. Immunohistochemistry was performed for the following antibodies to: Celsr1 (gift from C. Formstone, King's College London), nephrin (Progen Biotechnik, Heidelberg, Germany), proliferating cell nuclear antigen (PCNA; BD Biosciences, Oxford, UK), phospho-histone H3 (pH3; Millipore, Dundee, UK), Cleaved caspase-3 (Cell Signalling Technology, Danvers, MA, USA), rhodamine-conjugated phalloidin (Invitrogen, Paisley, UK), Scrib (Santa Cruz Biotechnology, USA), synaptopodin (Acris, Herford, Germany) and WT-1 (Acris). Bound antibodies were detected with either Alexa Fluor 488 or 594 secondary antibodies or appropriate horse-radish-conjugated antibodies followed by diaminobenzidine detection. Cell nuclei were visualized by staining with 4′,6-diamidino-2-phenylindole (DAPI, HCl). As negative controls, primary antibodies were omitted.

Explant culture and whole-mount metanephros staining

Freshly isolated metanephroi were collected from *Vangl2*^{Lp} homozygotes and wild-type littermates. Some metanephroi were used immediately for staining but others were cultured for up to 5 days as described (32). Metanephroi were fixed and incubated with anti-pan-cytokeratin (Sigma) and/or anti-WT1, followed by appropriate Alexa Fluor 488 or 594 secondary antibodies. Explants were imaged using confocal microscopy and the number of tubules in each explant counted.

Urine analysis

Twelve-week-old male *Vangl2*^{Lp} heterozygote and wild-type littermates were individually housed in metabolic cages for 24 h for urine collection. Urine concentration of albumin (Exocell Incorporation, Philadelphia, PA, USA) and retinal-binding protein-4 (Alpco Diagnostics, Salem, OR, USA) were assessed using commercially available kits according to the manufacturer's protocols. All data were normalized to urinary creatinine concentrations, measured by an Olympus Au400 autoanalyser.

Glomerular morphology and counts

Glomerular morphology was assessed according to the following categories: a, normal; b, only one or two capillary loops; c, no capillary loops; d, abnormal. Glomeruli from E18.5 kidney sections from wild-type, *Vangl2*$^{Lp/+}$ and *Vangl2*$^{Lp/Lp}$ mice were photographed and assigned to each category by an assessor unaware of the genotypes. At least 100 glomeruli in each of three kidneys from each of the three genotypes were assessed. In individual kidneys, care was taken to use sections at least 100 μm from each other to avoid counting the same glomeruli more than once. For each kidney, the proportion of glomeruli in each category was then calculated. Results are expressed as a percentage of total glomeruli in each genotype. The same images were used to calculate glomerular tuft diameters (which was taken as the maximum diameter of each tuft). To measure the number of glomeruli in each kidney, organs were removed from 4-week-old heterozygote *Vangl2*^{Lp} and wild-type male mice and placed in 0.1 M hydrochloric acid for 30 min at 37°C. The acid was removed and replaced with PBS and the tissue homogenized. Twenty lmicrolitres of this was pipetted into a haemacytometer and using a 10× objective lens, the number of glomeruli in the aliquot counted. This was repeated in triplicate for each sample and the three results averaged to determine the number of glomeruli in each sample and therefore each kidney (65).

Podocyte cell culture

Mouse podocytes (gift from Peter Mundel, University of Miami, USA) (37) were cultured on tissue culture plastic coated with 1% Matrigel substrate. For ongoing proliferation, cells were cultured at 33°C in a 5% CO_2 incubator in RPMI (Invitrogen) supplemented with 10% FCS (Invitrogen), antibiotics and interferon-γ (10 U/ml). To induce differentiation, cells were thermoshifted to 37°C and cultured in RPMI in the absence of interferon-γ. Cells were allowed to differentiate under these conditions for 7 days when they formed extensive processes similar to their *in vivo* phenotype.

Quantitative RT–PCR

One mg of RNA was isolated from proliferating and differentiating podocytes using TRI Reagent and cDNA prepared for PCR of the PCP genes *Celsr1*, *Fat4*, *Mpk1*, *Mpk2*, *Vangl1* and *Vangl2* using previously described methods (66). To assess differences in gene expression, quantitative real-time RT–PCR was performed (66) on samples from three independent experiments. All measurements were performed in duplicate and HPRT was used as a housekeeping gene to allow quantification. Alterations in gene expression in differentiated cells were expressed relative to the mean intensity in undifferentiated cells which was given a standardized value of 1. Negative controls of reactions without cDNA template were included. Primer details are available on request.

Statistical methods

Data were analysed using either unpaired two-tailed *t*-tests, or when more than two groups were analysed by one-way ANOVA with least square difference correction. Significance was accepted at $P < 0.05$; error bars in all data represent standard error mean.

SUPPLEMENTARY MATERIAL

Supplementary Material is available at *HMG* online.

ACKNOWLEDGEMENTS

We thank Caroline Formstone for providing Celsr1 antibody, Peter Mundel for the mouse podocyte cell line and Lauren Chessum for technical assistance.

Conflict of Interest statement. None declared.

FUNDING

This work was supported by the Medical Research Council, the NIHR Manchester Biomedical Research Centre, St Peter's Trust for Kidney Bladder & Prostate Research, the Wellcome Trust, a Walport/NIHR clinical lecturership to J.P. and a Kidney Research UK Non-Clinical Senior Fellowship to D.A.L. Funding to pay the Open Access Charge was provided by Medical Research Council.

REFERENCES

1. Barrow, J.R. (2006) Wnt/PCP signaling: a veritable polar star in establishing patterns of polarity in embryonic tissues. *Semin. Cell Dev. Biol.*, **17**, 185–193.
2. Karner, C., Wharton, K.A. Jr. and Carroll, T.J. (2006) Planar cell polarity and vertebrate organogenesis. *Semin. Cell Dev. Biol.*, **17**, 194–203.
3. Lake, B.B. and Sokol, S.Y. (2009) Strabismus regulates asymmetric cell divisions and cell fate determination in the mouse brain. *J. Cell Biol.*, **185**, 59–66.
4. Le Grand, F., Jones, A.E., Seale, V., Scime, A. and Rudnicki, M.A. (2009) Wnt7a activates the planar cell polarity pathway to drive the symmetric expansion of satellite stem cells. *Cell Stem Cell*, **4**, 535–547.
5. Guirao, B., Meunier, A., Mortaud, S., Aguilar, A., Corsi, J.M., Strehl, L., Hirota, Y., Desoeuvre, A., Boutin, C., Han, Y.G. *et al.* (2010) Coupling between hydrodynamic forces and planar cell polarity orients mammalian motile cilia. *Nat. Cell Biol.*, **12**, 341–350.
6. Song, H., Hu, J., Chen, W., Elliott, G., Andre, P., Gao, B. and Yang, Y. (2010) Planar cell polarity breaks bilateral symmetry by controlling ciliary positioning. *Nature*, **466**, 378–382.
7. Torban, E., Wang, H.J., Patenaude, A.M., Riccomagno, M., Daniels, E., Epstein, D. and Gros, P. (2007) Tissue, cellular and sub-cellular localization of the Vangl2 protein during embryonic development: effect of the Lp mutation. *Gene Expr. Patterns*, **7**, 346–354.
8. Torban, E., Wang, H.J., Groulx, N. and Gros, P. (2004) Independent mutations in mouse Vangl2 that cause neural tube defects in looptail mice impair interaction with members of the Dishevelled family. *J. Biol. Chem.*, **279**, 52703–52713.
9. Gravel, M., Iliescu, A., Horth, C., Apuzzo, S. and Gros, P. (2010) Molecular and cellular mechanisms underlying neural tube defects in the loop-tail mutant mouse. *Biochemistry*, **49**, 3445–3455.
10. Murdoch, J.N., Doudney, K., Paternotte, C., Copp, A.J. and Stanier, P. (2001) Severe neural tube defects in the loop-tail mouse result from mutation of *Lpp1*, a novel gene involved in floor plate specification. *Hum. Mol. Genet.*, **10**, 2593–2601.
11. Ybot-Gonzalez, P., Savery, D., Gerrelli, D., Signore, M., Mitchell, C.E., Faux, C.H., Greene, N.D. and Copp, A.J. (2007) Convergent extension, planar-cell-polarity signalling and initiation of mouse neural tube closure. *Development*, **134**, 789–799.
12. Torban, E., Patenaude, A.M., Leclerc, S., Rakowiecki, S., Gauthier, S., Andelfinger, G., Epstein, D.J. and Gros, P. (2008) Genetic interaction between members of the Vangl family causes neural tube defects in mice. *Proc. Natl Acad. Sci. USA*, **105**, 3449–3454.
13. Doudney, K., Ybot-Gonzalez, P., Paternotte, C., Stevenson, R.E., Greene, N.D., Moore, G.E., Copp, A.J. and Stanier, P. (2005) Analysis of the planar cell polarity gene *Vangl2* and its co-expressed paralogue *Vangl1* in neural tube defect patients. *Am. J. Med. Genet. A*, **136**, 90–92.
14. Kibar, Z., Torban, E., McDearmid, J.R., Reynolds, A., Berghout, J., Mathieu, M., Kirillova, I., De Marco, P., Merello, E., Hayes, J.M. *et al.* (2007) Mutations in VANGL1 associated with neural-tube defects. *N. Engl. J. Med.*, **356**, 1432–1437.
15. Kibar, Z., Bosoi, C.M., Kooistra, M., Salem, S., Finnell, R.H., De Marco, P., Merello, E., Bassuk, A.G., Capra, V. and Gros, P. (2009) Novel mutations in VANGL1 in neural tube defects. *Hum. Mutat.*, **30**, E706–715.
16. Lei, Y.P., Zhang, T., Li, H., Wu, B.L., Jin, L. and Wang, H.Y. (2010) VANGL2 mutations in human cranial neural-tube defects. *N. Engl. J. Med.*, **362**, 2232–2235.
17. Reynolds, A., McDearmid, J.R., Lachance, S., De Marco, P., Merello, E., Capra, V., Gros, P., Drapeau, P. and Kibar, Z. (2010) VANGL1 rare variants associated with neural tube defects affect convergent extension in zebrafish. *Mech. Dev.*, **127**, 385–392.
18. Ross, A.J., May-Simera, H., Eichers, E.R., Kai, M., Hill, J., Jagger, D.J., Leitch, C.C., Chapple, J.P., Munro, P.M., Fisher, S. *et al.* (2005) Disruption of Bardet–Biedl syndrome ciliary proteins perturbs planar cell polarity in vertebrates. *Nat. Genet.*, **37**, 1135–1140.
19. Ferrante, M.I., Romio, L., Castro, S., Collins, J.E., Goulding, D.A., Stemple, D.L., Woolf, A.S. and Wilson, S.W. (2009) Convergent extension movements and ciliary function are mediated by ofd1, a zebrafish orthologue of the human oral-facial-digital type 1 syndrome gene. *Hum. Mol. Genet.*, **18**, 289–303.

20. Borovina, A., Superina, S., Voskas, D. and Ciruna, B. (2010) Vangl2 directs the posterior tilting and asymmetric localization of motile primary cilia. *Nat. Cell Biol.*, **12**, 407–412.
21. Costantini, F. and Kopan, R. (2010) Patterning a complex organ: branching morphogenesis and nephron segmentation in kidney development. *Dev. Cell*, **18**, 698–712.
22. Woolf, A. and Pitera, JE (2009) Embryology. In Avner, E.D., Harmon, W.E. and Niaudet, P. (eds), *Pediatric Nephrology*, 6th edn. Springer, New York, NY, pp. 3–30.
23. Quaggin, S.E. and Kreidberg, J.A. (2008) Development of the renal glomerulus: good neighbors and good fences. *Development*, **135**, 609–620.
24. Patrakka, J. and Tryggvason, K. (2010) Molecular make-up of the glomerular filtration barrier. *Biochem. Biophys. Res. Commun.*, **396**, 164–169.
25. Ashworth, S.L., Sandoval, R.M., Hosford, M., Bamburg, J.R. and Molitoris, B.A. (2001) Ischemic injury induces ADF relocalization to the apical domain of rat proximal tubule cells. *Am. J. Physiol. Renal Physiol.*, **280**, F886–F894.
26. Yates, L.L., Schnatwinkel, C., Murdoch, J.N., Bogani, D., Formstone, C.J., Townsend, S., Greenfield, A., Niswander, L.A. and Dean, C.H. (2010) The PCP genes *Celsr1* and *Vangl2* are required for normal lung branching morphogenesis. *Hum. Mol.Genet.*, **19**, 2251–2267.
27. Babayeva, S., Zilber, Y. and Torban, E. (2010) Planar cell polarity pathway regulates actin rearrangement, cell shape, motility and nephrin distribution in podocytes. *Am. J. Physiol. Renal Physiol*. June 10, 2010 (Epub ahead of print).
28. Hunt, G.M. and Whitaker, R.H. (1987) The pattern of congenital renal anomalies associated with neural-tube defects. *Dev. Med. Child Neurol.*, **29**, 91–95.
29. Robson, W.L., Leung, A.K. and Sinclair, O. (1991) Congenital urinary anomalies associated with neural tube defects. *Pediatr. Nephrol.*, **5**, 369.
30. Mandell, G.A., Maloney, K., Sherman, N.H. and Filmer, B. (1996) The renal axes in spina bifida: issues of confusion and fusion. *Abdom. Imaging*, **21**, 541–545.
31. Kobayashi, A., Valerius, M.T., Mugford, J.W., Carroll, T.J., Self, M., Oliver, G. and McMahon, A.P. (2008) Six2 defines and regulates a multipotent self-renewing nephron progenitor population throughout mammalian kidney development. *Cell Stem Cell*, **3**, 169–181.
32. Chan, S.K., Riley, P.R., Price, K.L., McElduff, F., Winyard, P.J., Welham, S.J., Woolf, A.S. and Long, D.A. (2009) Corticosteroid-induced kidney dysmorphogenesis is associated with deregulated expression of known cystogenic molecules, as well as Indian hedgehog. *Am. J. Physiol. Renal Physiol.*, **298**, F346–356.
33. Guo, J.K., Menke, A.L., Gubler, M.C., Clarke, A.R., Harrison, D., Hammes, A., Hastie, N.D. and Schedl, A. (2002) WT1 is a key regulator of podocyte function: reduced expression levels cause crescentic glomerulonephritis and mesangial sclerosis. *Hum. Mol. Genet.*, **11**, 651–659.
34. Murdoch, J.N., Henderson, D.J., Doudney, K., Gaston-Massuet, C., Phillips, H.M., Paternotte, C., Arkell, R., Stanier, P. and Copp, A.J. (2003) Disruption of scribble (Scrb1) causes severe neural tube defects in the circletail mouse. *Hum. Mol. Genet.*, **12**, 87–98.
35. Montcouquiol, M., Sans, N., Huss, D., Kach, J., Dickman, J.D., Forge, A., Rachel, R.A., Copeland, N.G., Jenkins, N.A., Bogani, D. *et al.* (2006) Asymmetric localization of Vangl2 and Fz3 indicate novel mechanisms for planar cell polarity in mammals. *J. Neurosci.*, **26**, 5265–5275.
36. Formstone, C.J., Moxon, C., Murdoch, J., Little, P. and Mason, I. (2010) Basal enrichment within neuroepithelia suggests novel function(s) for Celsr1 protein. *Mol. Cell. Neurosci.*, **44**, 210–222.
37. Mundel, P., Reiser, J., Zuniga Mejia Borja, A., Pavenstadt, H., Davidson, G.R., Kriz, W. and Zeller, R. (1997) Rearrangements of the cytoskeleton and cell contacts induce process formation during differentiation of conditionally immortalized mouse podocyte cell lines. *Exp. Cell Res.*, **236**, 248–258.
38. Okuda, H., Miyata, S., Mori, Y. and Tohyama, M. (2007) Mouse Prickle1 and Prickle2 are expressed in postmitotic neurons and promote neurite outgrowth. *FEBS Lett.*, **581**, 4754–4760.
39. Tao, H., Suzuki, M., Kiyonari, H., Abe, T., Sasaoka, T. and Ueno, N. (2009) Mouse prickle1, the homolog of a PCP gene, is essential for epiblast apical-basal polarity. *Proc. Natl Acad. Sci. USA*, **106**, 14426–14431.
40. Asanuma, K., Yanagida-Asanuma, E., Faul, C., Tomino, Y., Kim, K. and Mundel, P. (2006) Synaptopodin orchestrates actin organization and cell motility via regulation of RhoA signalling. *Nat. Cell Biol.*, **8**, 485–491.
41. Goto, K. and Ishikawa, H. (1998) Differential distribution of actin and cytokeratin in isolated full-length rabbit renal tubules. *Cell Struct. Funct.*, **23**, 73–84.
42. Karner, C.M., Chirumamilla, R., Aoki, S., Igarashi, P., Wallingford, J.B. and Carroll, T.J. (2009) Wnt9b signaling regulates planar cell polarity and kidney tubule morphogenesis. *Nat. Genet.*, **41**, 793–799.
43. Fischer, E., Legue, E., Doyen, A., Nato, F., Nicolas, J.F., Torres, V., Yaniv, M. and Pontoglio, M. (2006) Defective planar cell polarity in polycystic kidney disease. *Nat. Genet.*, **38**, 21–23.
44. McNeill, H. (2009) Planar cell polarity and the kidney. *J. Am. Soc. Nephrol.*, **20**, 2104–2111.
45. Saburi, S., Hester, I., Fischer, E., Pontoglio, M., Eremina, V., Gessler, M., Quaggin, S.E., Harrison, R., Mount, R. and McNeill, H. (2008) Loss of Fat4 disrupts PCP signaling and oriented cell division and leads to cystic kidney disease. *Nat. Genet.*, **40**, 1010–1015.
46. Simons, M., Gloy, J., Ganner, A., Bullerkotte, A., Bashkurov, M., Kronig, C., Schermer, B., Benzing, T., Cabello, O.A., Jenny, A. *et al.* (2005) Inversin, the gene product mutated in nephronophthisis type II, functions as a molecular switch between Wnt signaling pathways. *Nat. Genet.*, **37**, 537–543.
47. Jones, C., Roper, V.C., Foucher, I., Qian, D., Banizs, B., Petit, C., Yoder, B.K. and Chen, P. (2008) Ciliary proteins link basal body polarization to planar cell polarity regulation. *Nat. Genet.*, **40**, 69–77.
48. GenitoUrinary Development Molecular Anatomy Project (GUDMAP). http://www.gudmap.org.
49. Olson, M.F. (2008) Applications for ROCK kinase inhibition. *Curr. Opin. Cell Biol.*, **20**, 242–248.
50. Michael, L., Sweeney, D.E. and Davies, J.A. (2005) A role for microfilament-based contraction in branching morphogenesis of the ureteric bud. *Kidney Int.*, **68**, 2010–2018.
51. Meyer, T.N., Schwesinger, C., Sampogna, R.V., Vaughn, D.A., Stuart, R.O., Steer, D.L., Bush, K.T. and Nigam, S.K. (2006) Rho kinase acts at separate steps in ureteric bud and metanephric mesenchyme morphogenesis during kidney development. *Differentiation*, **74**, 638–647.
52. Korostylev, A., Worzfeld, T., Deng, S., Friedel, R.H., Swiercz, J.M., Vodrazka, P., Maier, V., Hirschberg, A., Ohoka, Y., Inagaki, S. *et al.* (2008) A functional role for semaphorin 4D/plexin B1 interactions in epithelial branching morphogenesis during organogenesis. *Development*, **135**, 3333–3343.
53. Oxburgh, L., Chu, G.C., Michael, S.K. and Robertson, E.J. (2004) TGFbeta superfamily signals are required for morphogenesis of the kidney mesenchyme progenitor population. *Development*, **131**, 4593–4605.
54. Loughna, S., Hardman, P., Landels, E., Jussila, L., Alitalo, K. and Woolf, A.S. (1997) A molecular and genetic analysis of renal glomerular capillary development. *Angiogenesis*, **1**, 84–101.
55. Faul, C., Asanuma, K., Yanagida-Asanuma, E., Kim, K. and Mundel, P. (2007) Actin up: regulation of podocyte structure and function by components of the actin cytoskeleton. *Trends Cell Biol.*, **17**, 428–437.
56. Ichimura, K., Kurihara, H. and Sakai, T. (2010) Primary cilia disappear in rat podocytes during glomerular development. *Cell Tissue Res.*, **341**, 197–209.
57. Dai, C., Stolz, D.B., Kiss, L.P., Monga, S.P., Holzman, L.B. and Liu, Y. (2009) Wnt/beta-catenin signaling promotes podocyte dysfunction and albuminuria. *J. Am. Soc. Nephrol.*, **20**, 1997–2008.
58. Yokoi, H., Kasahara, M., Mukoyama, M., Mori, K., Kuwahara, K., Fujikura, J., Arai, Y., Saito, Y., Ogawa, Y., Kuwabara, T. *et al.* (2010) Podocyte-specific expression of tamoxifen-inducible Cre recombinase in mice. *Nephrol. Dial. Transplant.*, **25**, 2120–2124.
59. Yuan, H.T., Suri, C., Landon, D.N., Yancopoulos, G.D. and Woolf, A.S. (2000) Angiopoietin-2 is a site-specific factor in differentiation of mouse renal vasculature. *J. Am. Soc. Nephrol.*, **11**, 1055–1066.
60. Welham, S.J., Riley, P.R., Wade, A., Hubank, M. and Woolf, A.S. (2005) Maternal diet programs embryonic kidney gene expression. *Physiol. Genomics*, **22**, 48–56.
61. Cullen-McEwen, L.A., Kett, M.M., Dowling, J., Anderson, W.P. and Bertram, J.F. (2003) Nephron number, renal function, and arterial pressure in aged GDNF heterozygous mice. *Hypertension*, **41**, 335–340.

62. Keller, G., Zimmer, G., Mall, G., Ritz, E. and Amann, K. (2003) Nephron number in patients with primary hypertension. *N. Engl. J. Med.*, **348**, 101–108.
63. Zhang, Z., Quinlan, J., Hoy, W., Hughson, M.D., Lemire, M., Hudson, T., Hueber, P.A., Benjamin, A., Roy, A., Pascuet, E. *et al.* (2008) A common RET variant is associated with reduced newborn kidney size and function. *J. Am. Soc. Nephrol.*, **19**, 2027–2034.
64. Kibar, Z., Vogan, K.J., Groulx, N., Justice, M.J., Underhill, D.A. and Gros, P. (2001) Ltap, a mammalian homolog of *Drosophila* Strabismus/Van Gogh, is altered in the mouse neural tube mutant Loop-tail. *Nat. Genet.*, **28**, 251–255.
65. Welham, S.J., Wade, A. and Woolf, A.S. (2002) Protein restriction in pregnancy is associated with increased apoptosis of mesenchymal cells at the start of rat metanephrogenesis. *Kidney Int.*, **61**, 1231–1242.
66. Price, K.L., Long, D.A., Jina, N., Liapis, H., Hubank, M., Woolf, A.S. and Winyard, P.J. (2007) Microarray interrogation of human metanephric mesenchymal cells highlights potentially important molecules *in vivo*. *Physiol. Genomics*, **28**, 193–202.